J|A|C|S COMMUNICATIONS

Published on Web 05/28/2009

# Direct Measurement of Photoinduced Charge Separation Distances in Donor−Acceptor Systems for Artificial Photosynthesis Using OOP-ESEEM

Raanan Carmieli, Qixi Mi, Annie Butler Ricks, Emilie M. Giacobbe, Sarah M. Mickley, and Michael R. Wasielewski*

*Department of Chemistry and Argonne-Northwestern Solar Energy Research (ANSER) Center, Northwestern University, Evanston, Illinois 60208-3113*

Received April 9, 2009; E-mail: m-wasielewski@northwestern.edu

Molecular systems for artificial photosynthesis have successfully employed bioinspired, multistep electron transfer strategies to achieve long-lived radical ion pair (RP) states for solar energy conversion and storage.[1,2] The distance over which the two charges are separated depends on the structure of the molecular donor−acceptor array, while the lifetime of the charge separation and ultimately its ability to carry out useful redox chemistry depend on the electronic coupling between the final oxidized donor and reduced acceptor. The radical ions produced by charge separation are frequently delocalized over the $\pi$ systems of the final oxidized donor and reduced acceptor, so that there is often significant uncertainty as to the average distance between the separated charges, which in turn translates into uncertainty in the degree to which the radical ions are electronically coupled. In fact, in low dielectric constant media, where the Coulomb attraction of the ions may be significant, the charge distribution of the ions may be distorted, so that the average distance between them may be shorter than that implied by their chemical structures.[3,4]

Pulse EPR spectroscopy offers powerful methods to measure spin−spin interactions within photogenerated RPs, which directly yield structural information.[5] For example, the anisotropic dipolar interaction, $D$, between the unpaired electrons in the RP depends on the RP distance ($1/r^3$), while the exchange interaction ($J$) monitors the electronic coupling between the radicals.[6] The earliest application of electron spin echo (ESE) spectroscopy to photosynthetic reaction center (RC) proteins using a Hahn two-pulse echo experiment, $\pi/2$-$\tau$-$\pi$-$\tau$-echo, where $\tau$ is the delay time between the $\pi/2$ and $\pi$ microwave pulses, observed that the echo signal from the photogenerated RP is phase-shifted relative to that of the same spin system at thermal equilibrium and appears with the same phase as the applied microwave pulses.[7] Later theoretical studies showed that this "out-of-phase" (OOP) echo is due to the spin−spin interactions $D$ and $J$ within the RP, which modulate the echo decay as a function of $\tau$, so that the overall observed effect is termed out-of-phase electron spin echo envelope modulation (OOP-ESEEM).[8,9] The first experiments using OOP-ESEEM to determine $D$, and therefore the RP distance, were performed on the charge separated state within the RC of *Rb. sphaeroides* ($P_{865}^{+\bullet}Q_A^{-\bullet}$).[10] The RP distance derived from $D$ was found to agree very well with that obtained from the RC X-ray crystal structure.[11] While this approach has been successfully applied to a variety of RC proteins,[12−16] it has not been demonstrated for artificial photosynthetic systems. Here we show for the first time direct RP distance measurements in several artificial photosynthetic model systems using OOP-ESEEM.

The synthesis and characterization of electron donor−acceptor molecules **1**−**3** are reported in the Supporting Information. Photoexcitation of the charge transfer bands of 6ANI[17] in **1** and **2** and DMJ-An[18] in **3** rapidly produce the spin-correlated RPs **1**: $BDX^{+\bullet}$−$PI^{-\bullet}$, **2**: $TTF^{+\bullet}$−$PI^{-\bullet}$, and **3**: $DMJ^{+\bullet}$−$NI^{-\bullet}$. Samples for EPR measurements were dissolved in toluene (OD = 0.65 at 416 nm), loaded into 3.8 mm o.d. (2.4 mm i.d.) quartz tubes, subjected to several freeze−pump−thaw degassing cycles on a vacuum line ($10^{-4}$ Torr), and then flame-sealed using a hydrogen torch. Pulse EPR measurements were carried out using a Bruker Elexsys E580 spectrometer operating at 9.5 GHz (X-band). Samples were photoexcited at 85 K inside the EPR resonator using 416 nm, 0.7 mJ, 7 ns laser pulses at a 10 Hz repetition rate as described earlier.[19] The spin echo was generated using two microwave pulses following the laser pulse in the sequence: laser-$t_D$-$\pi/2$-$\tau$-$\pi$-$\tau$-echo, where $t_D$ = 200 ns, the $\pi/2$ and $\pi$ microwave pulses were 8 and 16 ns long, respectively. The echo signal was measured as a function of the delay time $\tau$ between the two microwave pulses (in increments of 12 ns beginning at $\tau$ = 108 ns). The spin-polarized EPR spectra of $BDX^{+\bullet}$−$PI^{-\bullet}$, $TTF^{+\bullet}$−$PI^{-\bullet}$, and $DMJ^{+\bullet}$−$NI^{-\bullet}$ obtained at 100 ns after the laser flash are given in Figure S1.

Figure 1 shows the time dependent OOP-ESEEM associated with the spin correlated RPs of **1**−**3**. As predicted by theory[8,9] and observed experimentally,[10] the out-of-phase echo decays show strong modulation. After orientational averaging, the time domain echo can be described by[15,16]

$$S(\tau) = Ae^{-\tau/T}\int_0^{2\pi}\int_0^{\pi}\sin(\omega\tau)\sin(\theta)\,d\theta\,d\phi \qquad (1)$$

where $T$ is the relaxation time, $A$ is the amplitude of the modulated echo, $\omega = 2J - 2D(\cos^2\theta - {}^1/_3)$, and $\theta$ is the angle between the externally applied magnetic field and the vector joining the two spins in the RP. The data in Figure 1 were least-squares fit to the analytical solution of eq 1, which yields $D$ and $J$ directly.[15,16] Since $A = 0$ for the spin-polarized RP when the delay time $\tau = 0$,[9] the echo amplitude during the initial 108 ns "dead time" was restored by extrapolating the fit of the modulation signal to $\tau = 0$. Sine Fourier transformation (SFT) of the fits to the data yield the spectra given in Figure 2. The SFT of the time domain modulation produces

 10.1021/ja902864h CCC: $40.75 

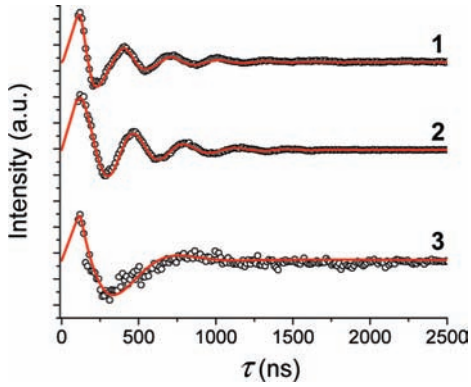


***Figure 1.*** Out-of-phase ESEEM of **1**−**3** measured at 85 K. Experimental conditions: (**1**) $\nu_{mw} = 9.714$ GHz, $B_0 = 345.8$ mT; (**2**) $\nu_{mw} = 9.614$ GHz, $B_0 = 342.3$ mT; (**3**) $\nu_{mw} = 9.716$ GHz, $B_0 = 346.0$ mT. The red traces are the fits to the experimental data.

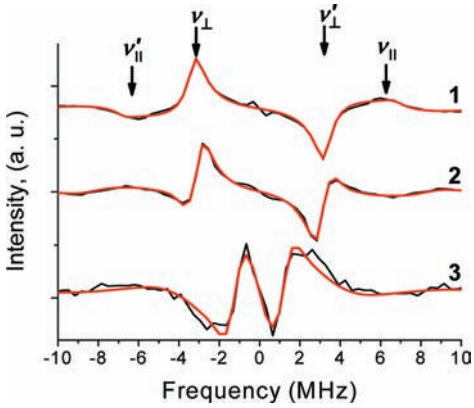


***Figure 2.*** Sine Fourier transformation (SFT) of the time domain echo modulation signals of **1**−**3** shown in Figure 1. The red curves superimposed on the experimental spectra are the SFTs of the fitting functions. The Pake doublet turning points are indicated.

***Table 1.*** Radical Pair Parameters and Distances for **1**−**3**

| | $D$ (μT) meas | $J$ (μT) meas | $r$ (Å) meas | $r$ (Å) calcd | $D$ (μT) calcd | $E$ (μT) calcd |
|---|---|---|---|---|---|---|
| **1** | $-179 \pm 2$ | $-18 \pm 2$ | $25.0 \pm 0.1$ | 25.4 | −144 | 0.8 |
| **2** | $-125 \pm 2$ | $12 \pm 2$ | $28.1 \pm 0.1$ | 27.3 | −108 | 0.4 |
| **3** | $-52 \pm 2$ | $7 \pm 2$ | $38.0 \pm 0.2$ | 37.6 | −47 | 0.0 |

a Pake doublet with turning points ($\nu_\perp$, $\nu_{||}$) and ($\nu'_\perp$, $\nu'_{||}$) resulting from the two dipolar- and exchanged-coupled spins having an antisymmetric shape with respect to the central frequency due to spin polarization. The peaks $\nu_\perp$ and $\nu'_\perp$ are assigned to perpendicular orientation of the vector connecting the radical ions within the RP with respect to the magnetic field ($\theta = 90°$), while the spectral edges $\nu_{||}$ and $\nu'_{||}$ are assigned to the parallel orientation ($\theta = 0°$). The RP distances were calculated using the point dipole approximation, $D = -2785$ mT·Å/$r^3$ (Table 1).

The measured RP distances for **1**−**3** are compared in Table 1 with the calculated distances between the centroids of the spin distributions of the oxidized donors $BDX^{+\bullet}$, $TTF^{+\bullet}$, and $DMJ^{+\bullet}$ and those of the reduced acceptors $PI^{-\bullet}$ and $NI^{-\bullet}$ determined using the semiempirical UHF-PM3 method.[20] The centroids calculated for $BDX^{+\bullet}$, $TTF^{+\bullet}$, $PI^{-\bullet}$, and $NI^{-\bullet}$ are all at the geometric centers of their structures, while that of $DMJ^{+\bullet}$ is in the middle of its C−N bond. The measured RP distances for **1** and **3** agree well with those of the calculations, while the measured distance for **2** is ∼0.8 Å longer than the calculated value, which may be due to the distribution of rotational conformers of TTF about the phenyl to which it is attached, which results from the "off-axis" attachment of the TTF relative to the rod-like structure of **2**. These results show that, despite the intrinsically nonpolar nature of the toluene glass at 85 K, the spin (and charge) distributions of the RPs are not significantly distorted by Coulomb attraction over these long distances. As a further check on the assumptions intrinsic to the point dipole approximation, the $D$ value and its corresponding rhombicity parameter $E$ were calculated from the spin distributions of each radical using the energy minimized structures of **1**−**3** (Table 1). The calculated values of $D$ are slightly smaller than the measured values, while the $E$ values are negligible, showing that the point dipole approximation is adequate for determining the RP distances relative to the accuracy of the distances derived from the molecular orbital calculations.

The small $J$ values for **1** and **2** result from a combination of structural features that reduce the electronic coupling between the two radicals of the RP: namely, the saturated piperidine ring, which interrupts $\pi$ orbital overlap; the fact that the HOMOs and LUMOs of all of the aromatic imides and diimide components have nodal planes that bisect the imide N atoms at which they are connected; and the nearly orthogonal orientation of the phenyl ring joining ANI and PI. The $J$ value for **3** is reduced by the long distance between the radical ions.

This study shows that OOP-ESEEM is well-suited for probing the detailed structural features of charge-separated intermediates that are essential to understanding how to design molecules that prolong charge separation for artificial photosynthesis.

**Acknowledgment.** This work was supported by the Chemical Sciences, Geosciences, and Biosciences Division, Office of Basic Energy Sciences, DOE under Grant No. DE-FG02-99ER14999.

**Supporting Information Available:** Experimental details including the synthesis and spectra of **1**−**3**. This material is available free of charge via the Internet at http://pubs.acs.org.

## References

(1) Gust, D.; Moore, T. A.; Moore, A. L. *Acc. Chem. Res.* **2001**, *34*, 40–48.
(2) Wasielewski, M. R. *J. Org. Chem.* **2006**, *71*, 5051–5066.
(3) Bleisteiner, B.; Marian, T.; Schneider, S.; Brouwer, A. M.; Verhoeven, J. W. *Phys. Chem. Chem. Phys.* **2001**, *3*, 5383–5392.
(4) Mi, Q.; Weiss, E. A.; Ratner, M. A.; Wasielewski, M. R. *Appl. Magn. Reson.* **2007**, *31*, 253–270.
(5) Schweiger, A.; Jeschke, G. *Principles of pulse electron paramagnetic resonance*; Oxford University Press: Oxford, 2001.
(6) Weiss, E. A.; Ratner, M. A.; Wasielewski, M. R. *J. Phys. Chem. A* **2003**, *107*, 3639–3647.
(7) Thurnauer, M. C.; Norris, J. R. *Chem. Phys. Lett.* **1980**, *76*, 557–561.
(8) Salikhov, K. M.; Kandrashkin, Y. E.; Salikhov, A. K. *Appl. Magn. Reson.* **1992**, *3*, 199–216.
(9) Tang, J.; Thurnauer, M. C.; Norris, J. R. *Chem. Phys. Lett.* **1994**, *219*, 283–290.
(10) Dzuba, S. A.; Gast, P.; Hoff, A. J. *Chem. Phys. Lett.* **1995**, *236*, 595–602.
(11) Allen, J. P.; Feher, G.; Yeates, T. O.; Komiya, H.; Rees, D. C. *Proc. Natl. Acad. Sci. U.S.A.* **1987**, *84*, 5730–5734.
(12) Hoff, A. J.; Gast, P.; Dzuba, S. A.; Timmel, C. R.; Fursman, C. E.; Hore, P. J. *Spectrochim. Acta, Part A* **1998**, *54A*, 2283–2293.
(13) Dzuba, S. A.; Hoff, A. J. *Biol. Magn. Reson.* **2000**, *19*, 569–596.
(14) Bittl, R.; Zech, S. G. *Biochim. Biophys. Acta Bioenerg.* **2001**, *1507*, 194–211.
(15) Santabarbara, S.; Kuprov, I.; Fairclough, W. V.; Purton, S.; Hore, P. J.; Heathcote, P.; Evans, M. C. W. *Biochemistry* **2005**, *44*, 2119–2128.
(16) Santabarbara, S.; Kuprov, I.; Hore, P. J.; Casal, A.; Heathcote, P.; Evans, M. C. W. *Biochemistry* **2006**, *45*, 7389–7403.
(17) Greenfield, S. R.; Svec, W. A.; Gosztola, D.; Wasielewski, M. R. *J. Am. Chem. Soc.* **1996**, *118*, 6767–6777.
(18) Dance, Z. E. X.; Ahrens, M. J.; Vega, A. M.; Ricks, A. B.; McCamant, D. W.; Ratner, M. A.; Wasielewski, M. R. *J. Am. Chem. Soc.* **2008**, *130*, 830–832.
(19) Chernick, E. T.; Mi, Q.; Kelley, R. F.; Weiss, E. A.; Jones, B. A.; Marks, T. J.; Ratner, M. A.; Wasielewski, M. R. *J. Am. Chem. Soc.* **2006**, *128*, 4356–4364.
(20) Stewart, J. J. P. *J. Comput. Chem.* **1989**, *10*, 209–220.

JA902864H